Supporting Information for Reveillaud et al. "Subseafloor microbial communities in hydrogen-rich vent fluids from hydrothermal systems along the Mid-Cayman Rise"

Methods: Sample Collection

In addition to vent fluid samples collected with the mat sampler, background seawater samples (no detectable hydrothermal signals) from 2300 m and 5000 m depth were collected via Niskin rosette deployed from the ship. Approximately 3 L of seawater was passed though Sterivex filter shipboard and the filter was preserved with RNALater.

Rocks covered in white filamentous microbes were collected at Piccard using the ROV manipulator and placed into a biological sample bin fitted with a lid. Following recovery of the samples on the ship, rock fragments were immersed in RNALater in a whirlpack bag, incubated for 24 hours at 4 °C to stabilize nucleic acids, and stored at -80 °C. Microbial filaments were then scraped off of the thawed rock using a sterile razor, placed into a microcentrifuge tube, and subsequently stored at -80 °C until DNA extraction.

Methods: 16S rRNA gene v6 Processing, Data and Statistical Analysis

QIIME 1.5 pipeline (Caporaso et al., 2010) was used for OTU clustering to calculate rarefaction curves and carry out other analyses. Even sequencing depth per sample was established by multiple rarefactions of the smallest sequencing depth, using a total of 20,000 bacterial reads and 44,000 archaeal reads per sample. Relative abundance was calculated as the count of reads (or percent of sample) belonging to a particular OTU. Reads were clustered into operational taxonomic units (OTUs) at 96% sequence identity level using USEARCH (Edgar, 2010), with the minimum word length parameter set to 30. Reads were assigned a taxonomy using the Global Assignment of Sequence Taxonomy (GAST, Huse et al., 2008) using the SILVA 111 database for reference (Quast et al., 2013).

OTU tables were standardized, square root transformed, and further analyzed using the analysis of similarity (ANOSIM) within PRIMER 6 version 6.1.13 software (PRIMER-E, Plymouth, UK). A distance matrix was constructed using Bray-Curtis similarity, and the null hypothesis that no difference in microbial community structure exists between pre-defined sample groups, e.g., the Von Damm and the Piccard site, was tested. Tests of sampling site influence employed 999 permutations. Significance was established with p-values less than or equal to 0.05. Nonmetric multidimensional scaling (MDS) ordination (2-dimensional representation of microbial community structure) was used with the Bray-Curtis distance measure on the bacterial and archaeal relative abundance matrix of the 96% similarity grouped OTUs.

Oligotyping of the three dominant groups- *Methanothermococcus*, *Archaeoglobus*, and *Sulfurovum*- was performed in order to explore ecological patterns at fine scale as described in Eren et al. (2013). GAST identified (Huse et al., 2008) high-quality Illumina V6 fragments were submitted to the Oligotyping pipeline version 1.1 (available from http://oligotyping.org). The details of total number of samples and reads analyzed, entropy components that identified oligotypes among reads following the initial entropy and oligotyping analysis are provided in the table below. To reduce noise, only oligotypes that occurred at least 100 times across all samples were included.

	Sulfurovum	Methanothermococcus	Archaeoglobus
Number of reads analyzed	1,698,134	1,608,325	2,325,331
Number of samples analyzed	19	16	17
Number of entropy components chosen	19	11	17
Number of reads represented after QC	1,683,487	1,602,056	2,319,116
Percentage of reads represented in results	99.14	99.61	99.73
Final number of quality controlled oligotypes	200	88	84
Min substantive abundance of an oligotype (-M)	100	100	100

Methods: 16S rRNA gene amplification, cloning, and sequencing

Thermocycling conditions consisted of an initial denaturation step at 94°C for 3 min, followed by 34 cycles at 94°C for 40 s, 55°C for 60 s, and 72°C for 2 min, followed by a final extension at 72°C for 10 min. PCR products were verified to be the correct size (ca. 1500bp) on a 1% agarose gel stained with ethidium bromide and photographed under UV light. PCR products were purified using the MinElute PCR Purification Kit (Qiagen) and the products analyzed on 0.8% agarose gel. Products were gel excised, purified, cloned, and sequenced bi-directionally as described in (Huber et al., 2009). Primer sequences were trimmed by hand using BioEdit (Hall, 1999). Sequence alignment and evolutionary analyses were conducted in MEGA (Tamura et al., 2011) with 1000 bootstrap replicates.

Methods: Quantitative PCR (qPCR)

Plasmid DNA was extracted from Axial Seamount low-temperature diffuse vent clone libraries, purified, and linearized using the WizardPlus SV Minipreps DNA Purification System (Promega). Standards were constructed by mixing equal amounts of four bacterial plasmids for the quantification of bacterial 16S rRNA gene and two archaeal plasmids for the quantification of archaeal 16S rRNA gene. Accession numbers for the archaeal standards are HQ636042.1 and HQ636052.1 and those for the four bacterial standards are KT778268 - KT778271. A 1:10 dilution series of the plasmid mixtures

beginning with an initial concentration of approximately 0.058 ng μL-1 for bacterial samples and 0.097 ng μL-1 for archaeal samples was used to produce standard curves with R2 values > 0.99 and efficiencies ranging from 86% to 105%. Each 20 μL reaction contained KAPA PROBE FAST ABI Prism® 2X qPCR Master Mix (Kapa Biosystems), forward and reverse primers at optimized concentrations of either 3 nM (Bacteria) or 4 nM (Archaea), optimized probe concentrations of either 2.5 nM (Bacteria) or 5.0 nM (Archaea), DEPC-treated water, and 2 μL of DNA template. Reactions were performed in triplicate with no template controls on a StepOne Plus Real Time PCR System (Applied Biosystems). Cycles began with initial denaturation for 3 min at 96 °C, followed by 40 cycles of 15 s at 96°C and 3 min at 59 °C. STEPONE software version 2.2.2 (Applied Biosystems) was used to analyze the results.

Methods: Modelling

The modelling approach was similar to Amend et al., 2011 and others (McCollom and Shock 1997; Shock and Holland, 2004). To describe the energy available for microbial growth we considered nine potential redox reactions,

aerobic sulfide oxidation: $H_2S + 2O_2 \longrightarrow SO_4^{2-} + H^+$

aerobic methane oxidation: $CH_4 + 2O_2 \longrightarrow CO_2 + 2H_2O$

aerobic iron oxidation: $4Fe^{2+} + 2O_2 + 10H_2O \longrightarrow 4FeOH_3 + 8H^+$

aerobic hydrogen oxidation reaction: $2H_2 + O_2 \longrightarrow 2H_2O$

hydrogenothrophic sulfate reduction: $4H_2 + SO_4^{2-} + 2H^+ \longrightarrow H_2S + 4H_2O$

hydrotenotrophic methanogenesis: $4H_2 + CO_2 \longrightarrow CH_4 + 2H_2O$

anaerobic oxidation of methane: $CH_4 + SO_4^{2-} + 2H^+ \longrightarrow CO_2 + H_2S + 2H_2O.$

sulfide supported denitrification: $NO_3^- + \frac{5}{8}H_2S \longrightarrow \frac{5}{8}SO_4^{2-} + \frac{1}{2}N_2 + \frac{1}{4}H^+ + \frac{1}{2}H_2O$

hydrogen supported denitrification: $NO_3^- + \frac{5}{2}H_2 + H^+ \longrightarrow \frac{1}{2}N_2 + 3H_2O$

However, because our metagenomic data cannot distinguish between sulfide and hydrogen supported denitrification, the available energy from these two reactions was combined and expressed simply as denitrification (DEN), leaving eight unique types of metabolism in the model. Energy available from sulfur reduction was not possible with this model because elemental sulfur was not measured in the end-member fluid. Therefore, we only present sulfate reduction in the thermodynamic modelling.

To calculate the Gibbs free energy available from each reaction, vent fluid composition was determined by considering mixing between a high temperature end member and seawater at a series of mixing ratios meant to mimic the incremental titration of small aliquots of high temperature hydrothermal fluid with seawater.

At each step in the titration, equilibrium speciation of the resulting mixture was performed using EQ3/6 geochemical modelling software. During these calculations, equilibration of all redox reactions and mineral precipitation was suppressed. End

member concentrations for the 6 comparison vents were taken from Amend et al., 2011 and those for Piccard and Von Damm are given by Reeves et al., 2014 and McDermott et al., 2015. At each mixing ratio the free energy of the redox reaction associated with each type of metabolism is calculated according to,

$$\Delta G_r = \Delta G_r^\circ + RT \ln Q_r \qquad (1)$$

where ΔG_r° is the standard Gibbs free energy of reaction, *R* is the ideal gas constant, *T* is the temperature and Q_r accounts for the chemical composition of the mixture and is given by,

$$Q_r = \prod a_i^{\nu_{i,r}} \qquad (2)$$

where a_i is the activity of the species *i* raised to its stoichiometric reaction coefficient, $\nu_{i,r}$. The standard Gibbs free energy of reaction (ΔG_r°) is calculated with the Helgeson-Kirkham-Flowers (HKF) equations of state (Helgeson et al., 1978, 1981) and the activities of aqueous charged species are calculated using the B-dot equation (Helgeson et al., 1981). The supporting thermodynamic database for these calculations was generated at 25 MPa using SUPCRT92 (Johnson et al., 1992) software that included thermodynamic data for minerals (Helgeson et al., 1978) and relevant aqueous inorganic species (Shock and Helgeson, 1988; Shock et al., 1989, 1997; Sverjensky et al., 1997). Once the free energy was calculated the total energy potentially available for each reaction was determined by multiplying (1) by the limiting reactant. Results are expressed on an energy density basis (kJ kg^{-1} of mixed fluid), in accordance with Osburn et al. 2014, who suggest this provides the most accurate description of the energy available to a microbial community. This is in contrast to Amend et al., 2011 who normalize their results to the hydrothermal fluid component of the mixture (kJ kg^{-1} vent fluid)

Methods: 16S rRNA gene sequence extraction from metagenomes

Reads were mapped to Silva SSU and LSU taxonomic databases (Release 108, Pruesse et al. 2007) using Bowtie2 (Langmead and Salzberg 2012, and a local alignment) to identify all rRNA in metagenomes. The 16S rRNA gene sequences were then identified by mapping the identified rRNA reads to the Greengenes 2011 taxonomic database (McDonald et al. 2012) using Bowtie2. 16S rRNA gene sequences were classified with Mothur (v 1.21, Schloass et al.2009) using the Silva taxonomic database mentioned above.

Methods: 16S rRNA gene global taxonomic comparisons

16S rRNA gene data from this study were compared to next-generation sequencing datasets from previous vent studies, including diffuse (Huber et al., 2007) and post-eruption "snowblower' vents (Meyer et al., 2013) from Axial Seamount, Juan de Fuca Ridge; Lau Basin sulfide chimneys (Zinger et al, 2011); Lost City carbonate chimneys (Brazelton et al., 2010); Guaymas Basin hydrothermal sediments (Biddle et al., 2012); Mariana Arc diffuse vents (Huber et al., 2010); and Mid-Atlantic Ridge (MAR) sulfide chimneys from Rainbow and Lucky Strike (Flores et al., 2011). All data were obtained from VAMPS (Huse et al., 2014; http://vamps.mbl.edu/diversity/diversity.php), except those from the MAR, which were provided by Anna-Louise Reysenbach. Because different regions of the 16S rRNA gene were amplified and different sequencing platforms were used to sequence the amplicons, 16S rRNA genes were taxonomically compared using the Global Assignment of Sequence Taxonomy (GAST; Huse et al., 2008) on the VAMPS platform to the genus level. All sequences were normalized by total number of sequences, transformed via square root, and used to calculate a distance matrix with the Bray-Curtis measure. Distance matrices were used to generate the hierarchical clustering dendrograms in PRIMER-E v.6.1.6 (Clarke and Gorley, 2006).

Table S1. Latitude, Longitude and name of samples from this study.

Vent Site: Vent Field	Sample	Latitude (North)	Longitude (West)
Fuzzy Rock 1, 2: Piccard, BVM	Rock_21A	18.547	-81.7184
Shrimp Gulley #1: Piccard, BSM	FS850	18.5466	-81.7177
Shrimp Gulley #2: Piccard, BSM	FS856	18.5466	-81.7177
Hot Chimlet: Piccard, BVM	FS851	18.5472	-81.7181
Shrimp Canyon: Piccard, BVM	FS852	18.5471	-81.7182
Base of Lung Snack: Piccard, BWM	FS853	18.5461	-81.7181
X-19 at BV #4: Piccard, BVM	FS854	18.5466	-81.7182
Shrimp Vegas: Piccard, BVM	FS855	18.5471	-81.7182
Old Man Tree: Von Damm	FS841	18.375	-81.7976
Ravelin #1: Von Damm	FS847	18.3752	-81.7973
Ravelin #2: Von Damm	FS842	18.3752	-81.7971
Hot Cracks #1: Von Damm	FS846	18.3749	-81.7975
Hot Cracks #2: Von Damm	FS843	18.375	-81.7974
Shrimp Hole: Von Damm	FS844	18.3747	-81.7973
White Castle: Von Damm	FS845	18.3769	-81.798
Ginger Castle: Von Damm	FS848	18.3769	-81.7979
Main Orifice: Von Damm	FS849	18.3767	-81.7981
Seawater: Off Axis Von Damm	CTD02-10	18.6584	-81.7751
Seawater: Off Axis Piccard	CTD02-03	18.6584	-81.7751

BVM, Beebe Vents Mound; BSM, Beebe Sea Mound; BWM, Beebe Woods Mound

Fig. S1. Map of Caribbean Sea, with blue diamond indicating the location of the Mid-Cayman Rise (inset). Von Damm and Piccard hydrothermal vent fields are shown in white diamonds.

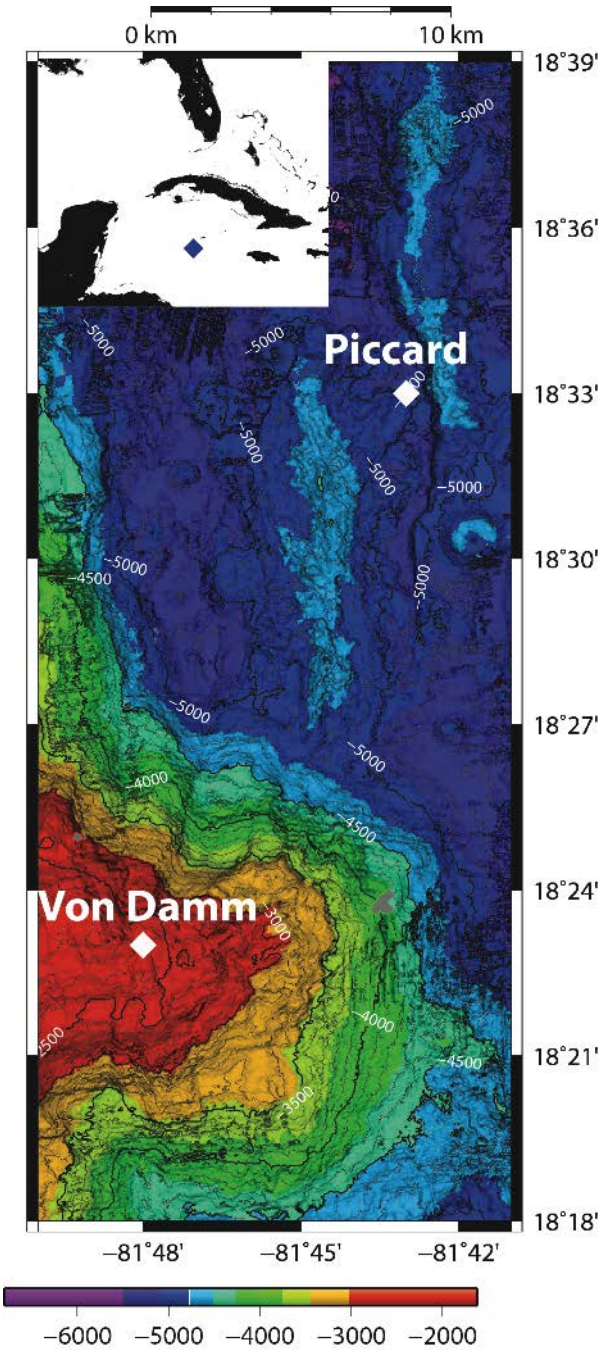

Fig. S2. ROV pictures of vent fluid sampling at selected vent site locations. A. Old Man Tree at Von Damm; B. Shrimp Hole at Von Damm; C. Shrimp Gulley at Piccard, Beebe Sea Mound; D. Fuzzy Rock at Piccard, Beebe Vents Mound.

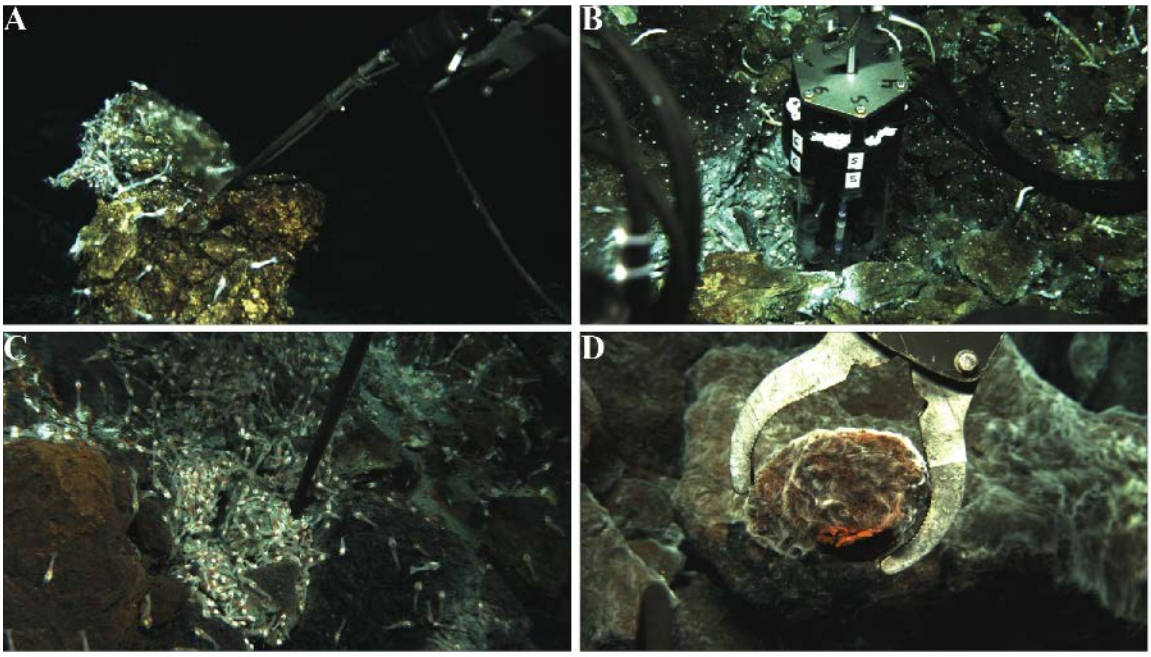

Fig. S3. DAPI stained epifluorescent micrographs of microorganisms found in venting fluids at (A) Shrimp Gulley #2, Piccard; (B) White Castle, Von Damm; (C) Hot Cracks #1, Von Damm; and (D) Shrimp Hole, Von Damm. All scale bars are 2 μm.

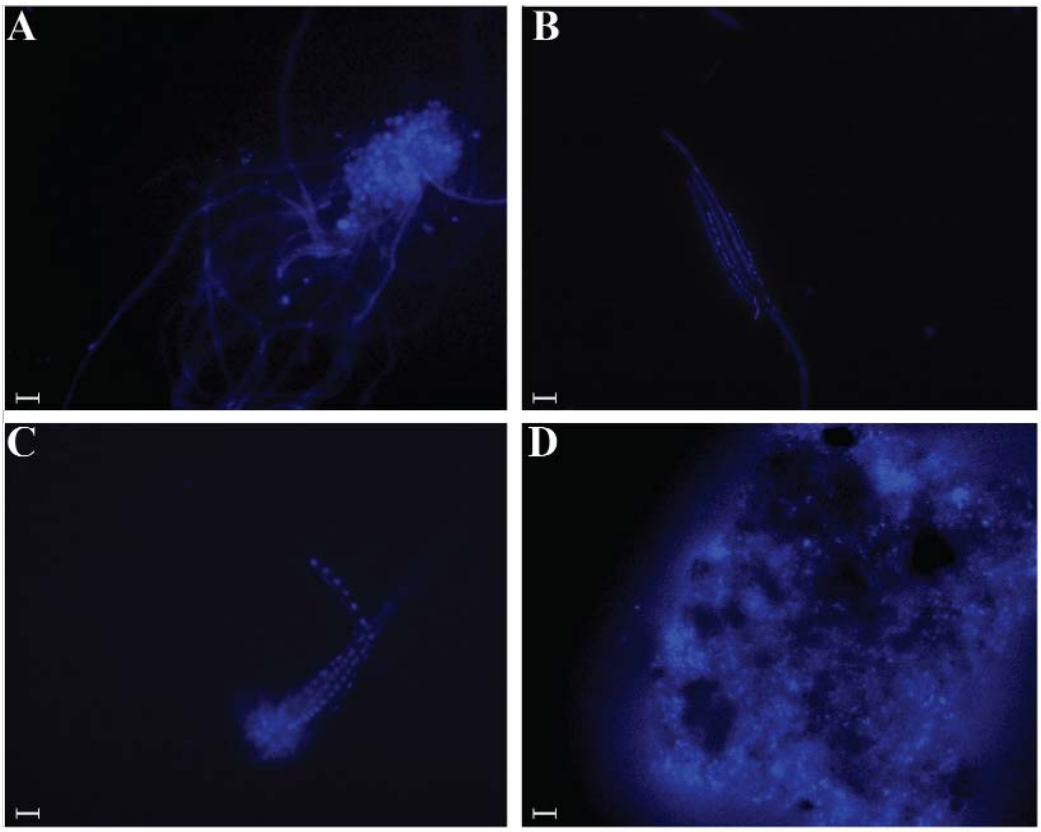

Fig. S4. MDS (Multidimensional Scaling) 2D similarity plot comparing all 16S rRNA gene 96% OTUs of (A) archaea and (B) bacteria, with each sample labeled according to vent field (Von Damm, filled circles; Piccard, open circles) and site name, including background seawater (filled squares) and Fuzzy Rock samples (open squares).

Fig. S5. Neighbor-joining tree of full-length 16S rRNA genes corresponding to *Archaeglobacae* sequences. Bootstrap values greater than 75 are indicated above branches. Sequences obtained in this study are highlighted in bold. The number of replicate clones is shown in parentheses.

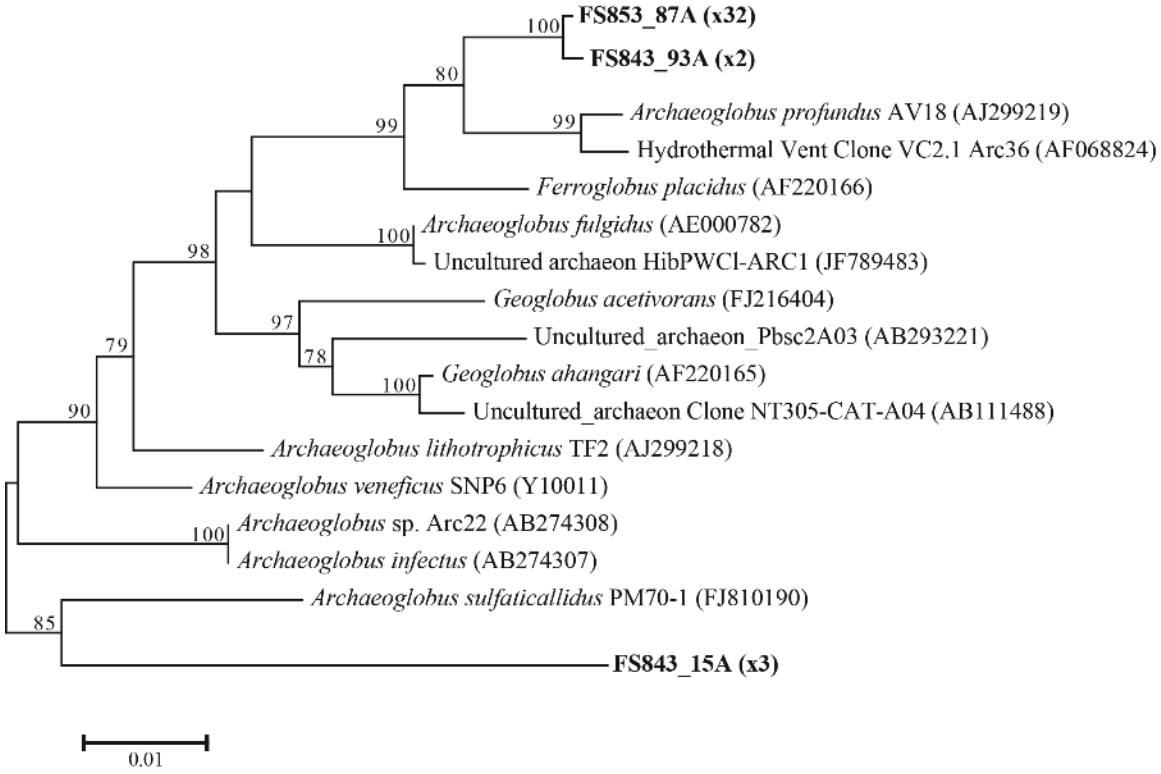

Fig. S6. MDS 2D similarity plot comparing 16S rRNA gene 96% OTUs of archaea, with each sample labeled according to vent field (Von Damm, filled circles; Piccard, open circles) and site name. Shrimp Hole is not included in the analysis.

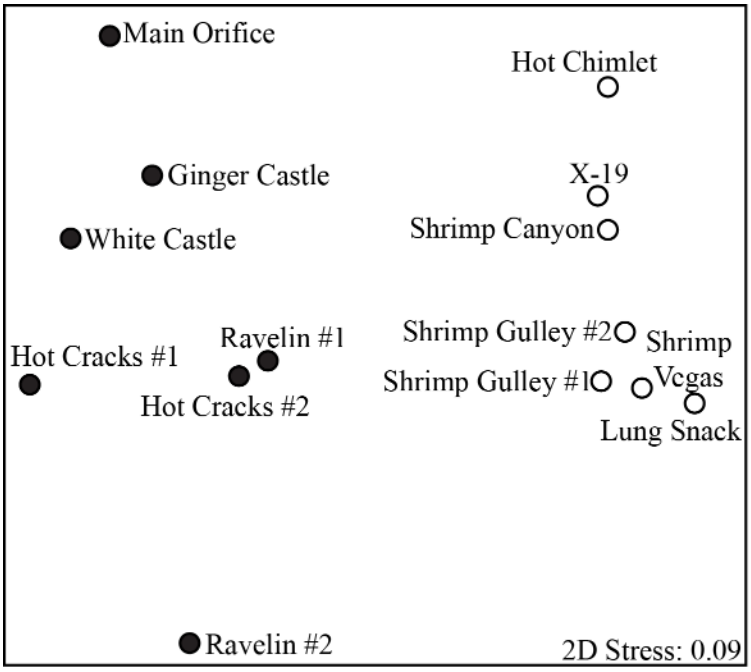

Fig. S7. Rarefaction curve at 96% OTUs of 16S rRNA genes for archaea at (A) Von Damm and (B) Piccard, with each sample labeled according to vent site name.

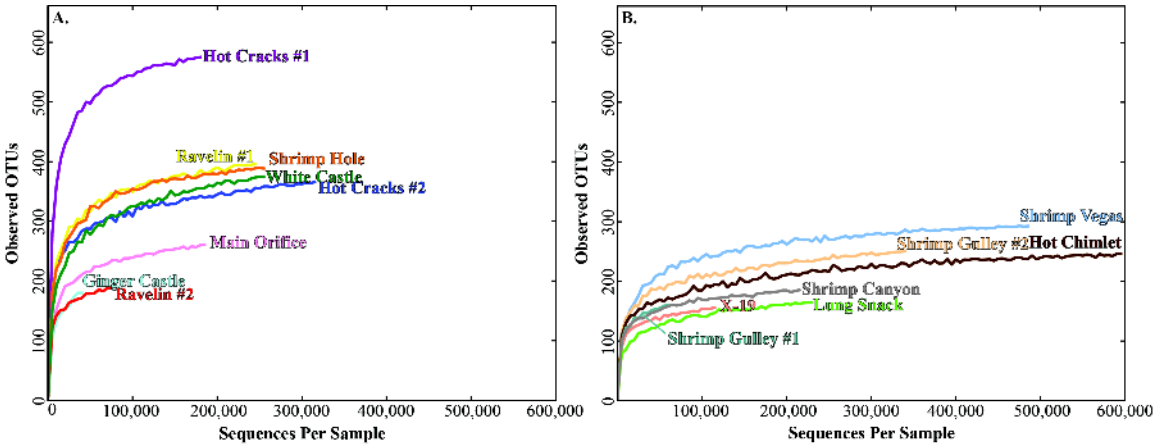

Fig. S8. Rarefaction curve at 96% OTUs of 16S rRNA genes for bacteria at (A) Von Damm and (B) Piccard, with each sample labeled according to vent site name.

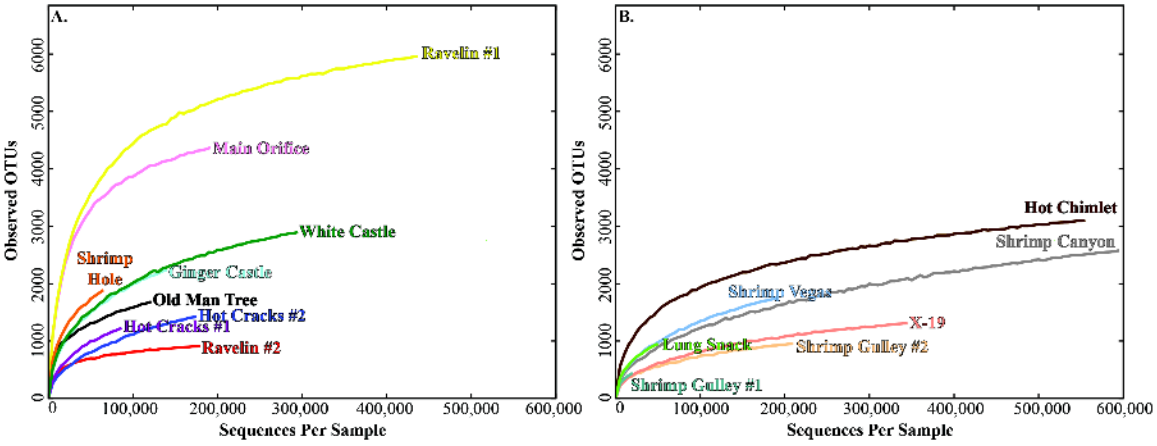

Fig S9. Cluster diagrams of community similarity based on taxonomy of bacterial 16S rRNA genes at the genus level (Left) and taxonomic diversity of bacterial communities (Right) for Piccard (PD), Von Damm (VD), Lau Basin sulfide chimneys (LAU), the Mid-Atlantic Ridge sulfide chimneys at Rainbow (RAIN) and Lucky Strike (LUCKY), Axial diffuse vent fluids (AXV) and post-eruption "snowblower' vent fluids (AXV-ER), Lost City carbonate chimneys (LCY), Guaymas Basin hydrothermal sediments (GMS), and Mariana Arc diffuse vent fluids (MARIANA).

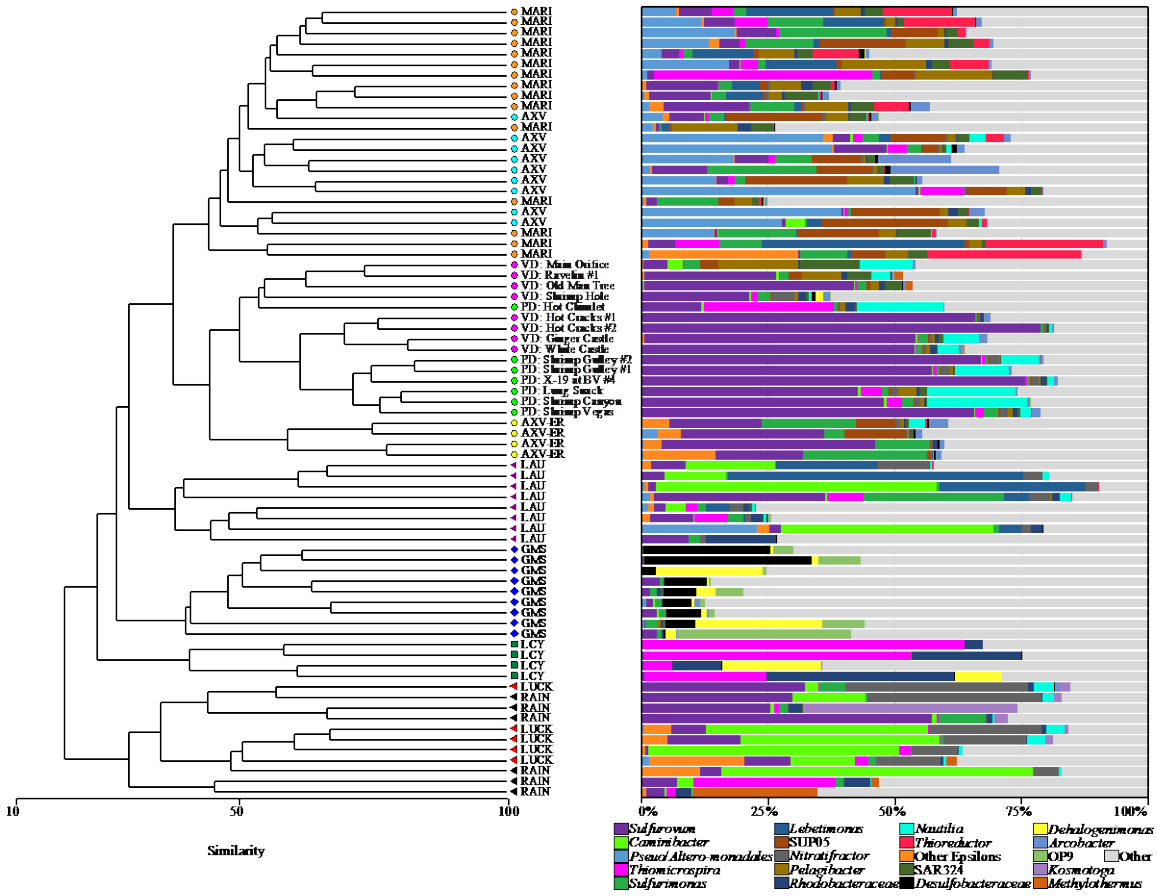

Fig. S10. Number of KEGGs ontology as a function of (A) frequency and (B) log transformed frequency at Von Damm and Piccard.

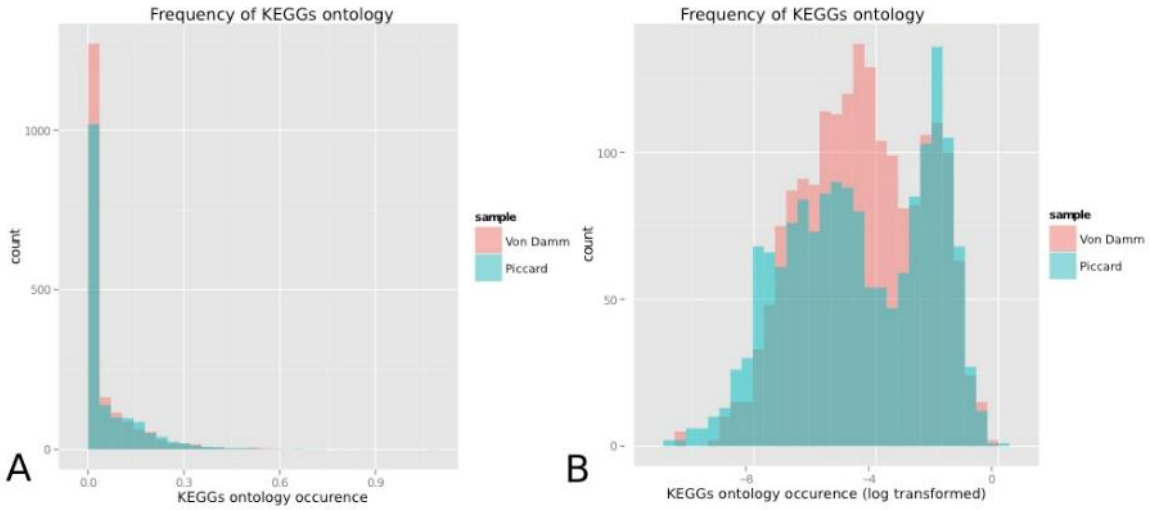

Fig. S11. Classification of 16S rRNA genes for (A) archaea and (B) bacteria identified from metagenomes for Ginger Castle (Von Damm) and Shrimp Gulley#2 (Piccard).

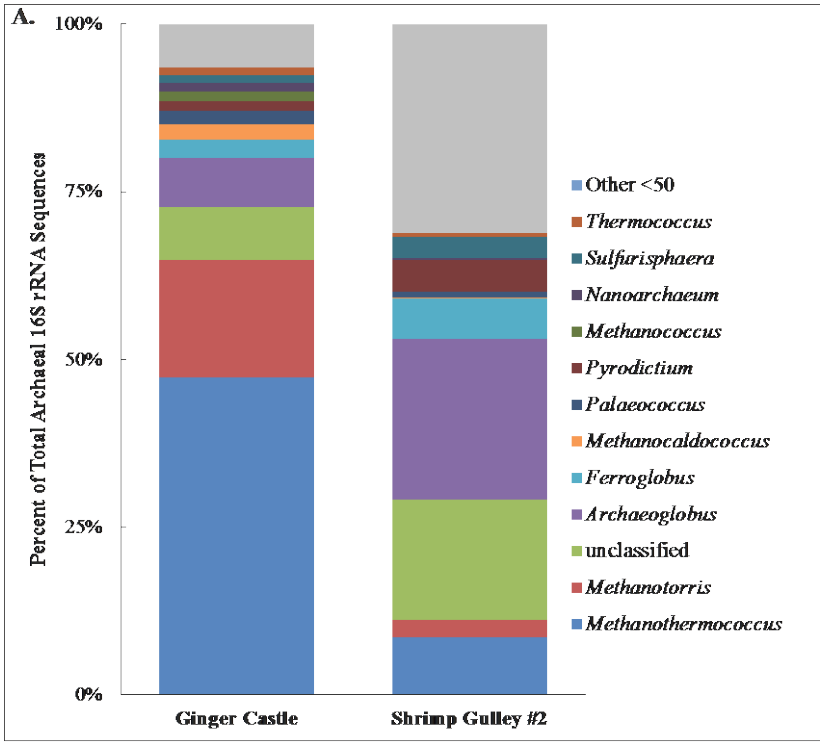

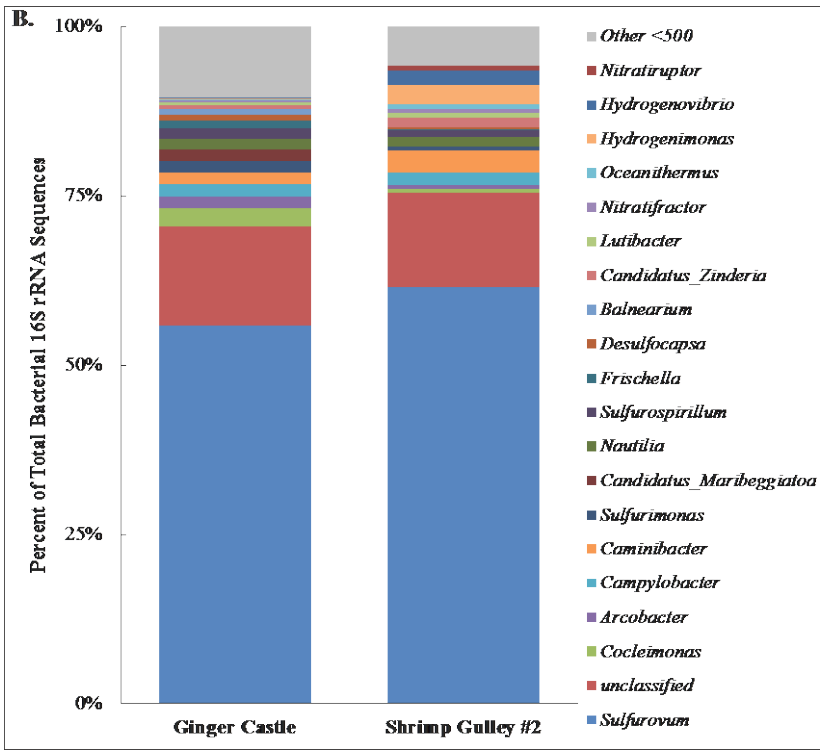

Fig. S12. Taxonomic annotation of key genes involved in hydrogen (green), methane (orange), nitrogen (purple), sulfur (blue), oxygen metabolism (grey) and in carbon fixation including Reductive TCA (red), Calvin Benson Bassham (yellow), 3-Hydroxpropionate/4-Hydroxybutyrate (cyan), and Reductive Acetyl-Coa (pink) at Von Damm and Piccard.

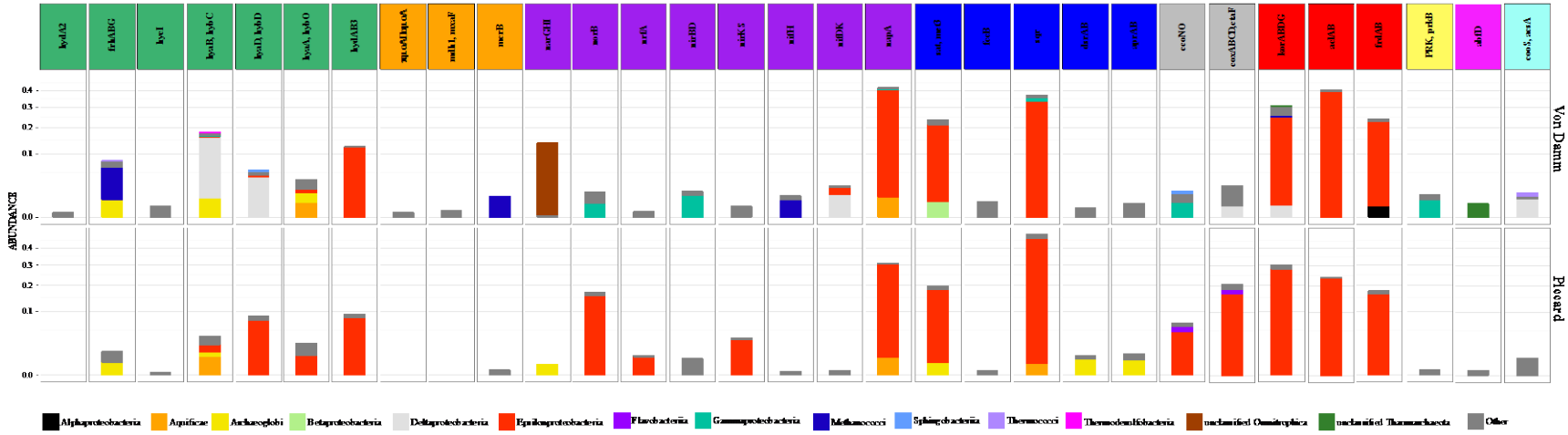

Fig. S13: COGs Relative abundances of major categories of functional genes in the shotgun metagenomes obtained from Von Damm (inner circle) and Piccard (outer circle).

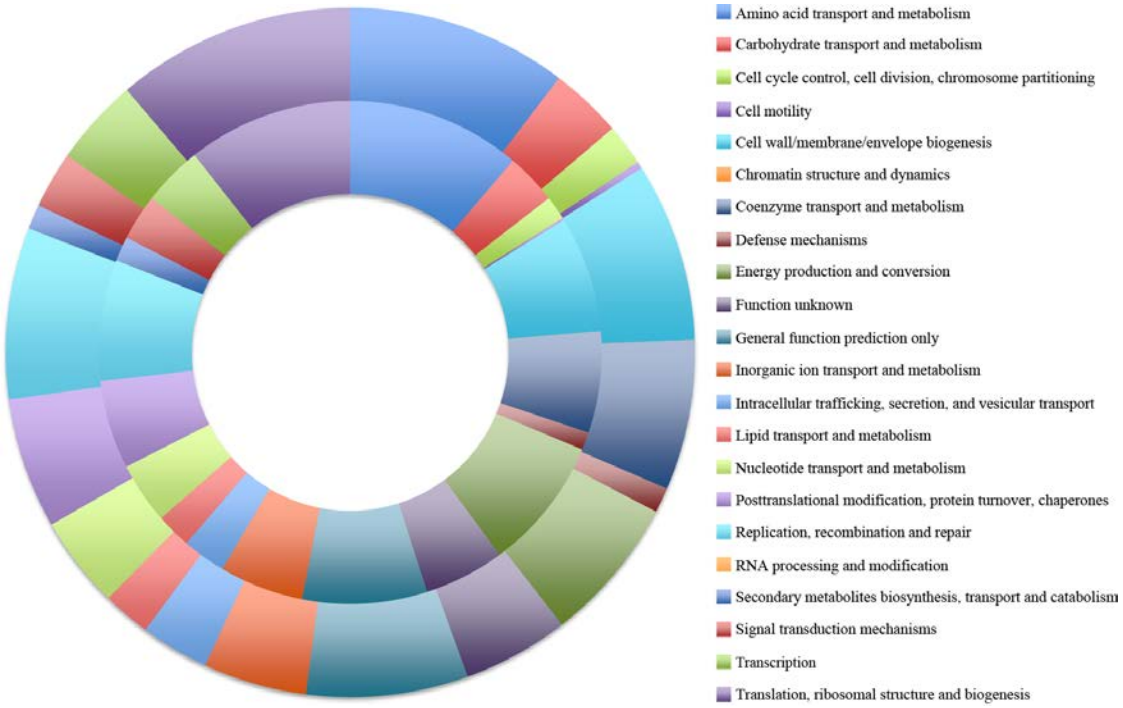

Fig. S14. Heat map showing the relative abundance of all KEGGs (Kyoto Encyclopedia of Genes and Genomes) in Von Damm and Piccard. The brightness (Yellow) in the heat map reflects the abundance (copies per genome) of a particular function in a sample.

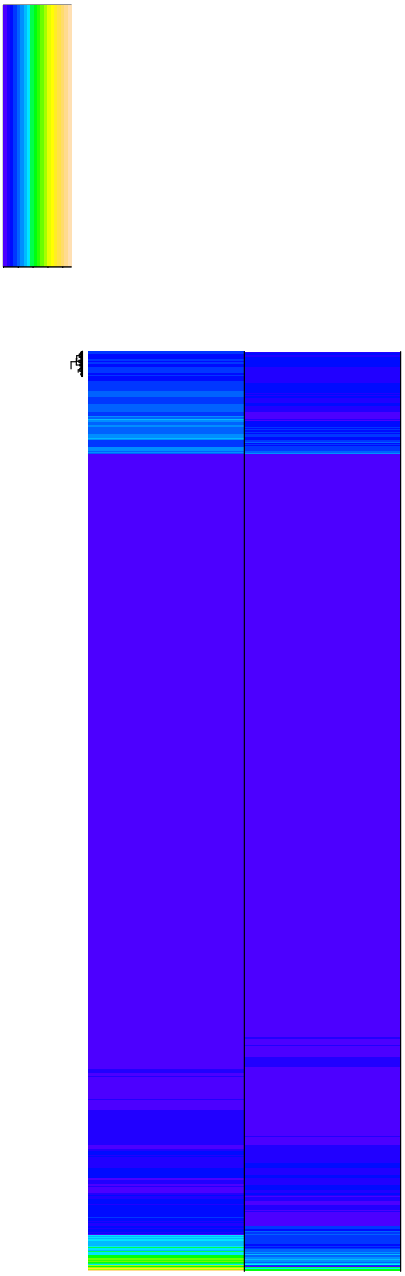

Fig. S15. Twenty most abundant functions in (A) Von Damm vs. Piccard and (B) Piccard vs. Von Damm annotated with KEGGS. The brightness (Yellow) in the heatmap reflects the abundance (copies per genome) of a particular function in a sample.

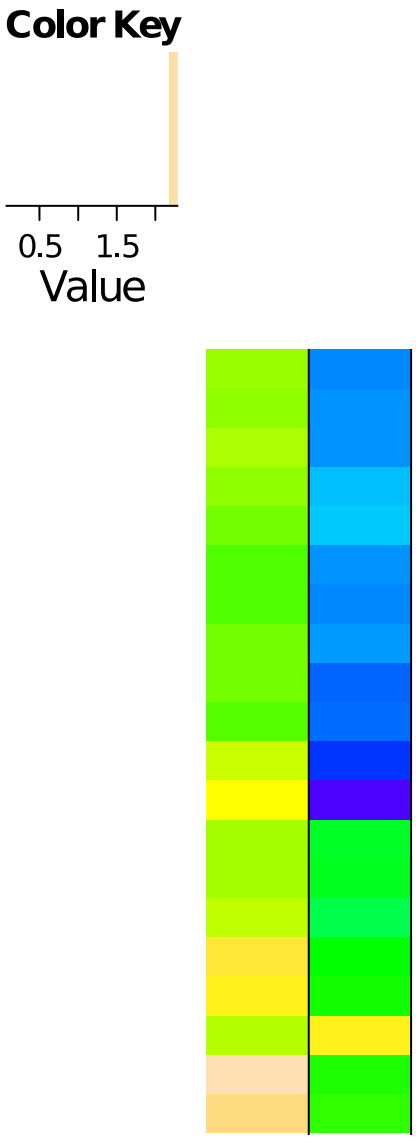

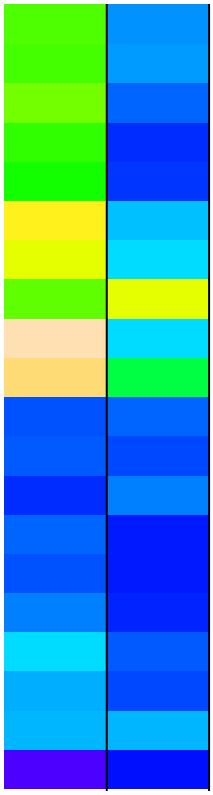

Carbamoyl–phosphate synthase large subunit (carB, CPA2)

methyltransferase 1 (DNMT1, dcm)

SI Text References

Amend, J.P., McCollom, T.M., Hentscher, M., and Bach, W. (2011) Catabolic and anabolic energy for chemolithoautotrophs in deep-sea hydrothermal systems hosted in different rock types. *Geochim Cosmochim Acta* **75**: 5736-5748.

Biddle, J.F., Cardman, Z., Mendlovitz, H., Albert, D.B., Lloyd, K.G., Boetius, A., *et al.* (2012) Anaerobic oxidation of methane at different temperature regimes in Guaymas Basin hydrothermal sediments. *ISME J* **6**: 1018–31.

Brazelton, W.J., Ludwig, K. a, Sogin, M.L., Andreishcheva, E.N., Kelley, D.S., Shen, C.-C., et al. (2010) Archaea and bacteria with surprising microdiversity show shifts in dominance over 1,000-year time scales in hydrothermal chimneys. *Proc. Natl. Acad. Sci. U. S. A* **107**: 1612–7.

Caporaso, J.G., Kuczynski, J., Stombaugh, J., Bittinger, K., Bushman, F.D., *et al.* (2010) QIIME allows analysis of high- throughput community sequencing data. *Nat Methods* **7**: 335–336.

Clarke, KR, Gorley, R. (2006) PRIMER v6: User Manual/Tutorial. PRIMER-E, Plymouth.

Edgar, R.C. (2010) Search and clustering orders of magnitude faster than BLAST. *Bioinformatics* **26**:2460–1.

Eren, A.M., Maignien, L., Sul, W.J., Murphy, L.G., Grim, S.L., Morrison, H.G., *et al.* (2013) Oligotyping : differentiating between closely related microbial taxa using 16S rRNA gene data. *Methods Ecol Evol* 1111–1119.

Flores G.E., Campbell, J.H., Kirshtein, J.D., Meneghin, J., Podar, M., *et al.* (2011) Microbial community structure of hydrothermal deposits from geochemically different vent fields along the Mid-Atlantic Ridge. *Environ Microbiol* **13**:2158–2171.

Hall, T. (1999) BioEdit: a user-friendly biological sequence alignment editor and analysis program for Windows 95/98/NT. *Nucleic Acids Symp.* Ser 01/1999 **41**:95-98.

Helgeson, H.C., Delany, J.M., Nesbitt, W.H., and Bird, D.K., (1978) Summary and critique of the thermodynamic properties of rock-forming minerals. *American Journal of Science* **278**: 1-229.

Helgeson, H.C., Kirkham, D.H., and Flowers, G.C., (1981) Theoretical prediction of the thermodynamic behavior of aqueous electrolytes at high pressures and temperatures: IV. Calculation of activity coefficients, osmotic coefficients, and apparent molal and standard and relative partial molal properties to 600°C and 5kb. *American Journal of Science* **281**: 1249-1516.

Huber, J.A., Mark Welch, D.B., Morrison, H.G., Huse, S.M., Neal, P.R., *et al.* (2007) Microbial population structures in the deep marine biosphere. *Science* **318**:97–100.

Huber, J.A., Morrison, H.G., Huse, S.M., Neal, P.R., Sogin, M.L., *et al.* (2009) Effect of PCR amplicon size on assessments of clone library microbial diversity and community structure. *Environ Microb* **11**:1292–302.

Huber, J.A., Cantin, H.V., Huse, S.M., Welch, D.B.M., Sogin, M.L, *et al.* (2010) Isolated communities of Epsilonproteobacteria in hydrothermal vent fluids of the Mariana Arc seamounts. *FEMS Microbiol Ecol* **73**:538–49.

Huse, S.M., Dethlefsen, L., Huber, J.A, Welch, D.M., Relman, D.A., *et al.* (2008) Exploring microbial diversity and taxonomy using SSU rRNA hypervariable tag sequencing. *PLoS Gen*. 4, e1000255.

Huse, S.M., Mark Welch, D.B., Voorhis, A., Shipunova, A., Morrison, H.G., *et al.* (2014) VAMPS: a website for visualization and analysis of microbial population structures. *BMC Bioinformatics **15**: 41*.

Johnson, J.W., Oelkers, E.H., and Helgeson, H.C. (1992) SUPCRT92: a software package for calculating the standard molal properties of minerals, gases, aqueous species, and reactions from 1 to 5000 bar and 0 to 1000ºC. *Computers and Geosciences* **28**: 899-947.

McDonald D, Price MN, Goodrich J, Nawrocki EP, DeSantis TZ, Probst A *et al* (2012). An improved Greengenes taxonomy with explicit ranks for ecological and evolutionary analyses of bacteria and archaea. *Isme J* **6:** 610-618.

McCollom, T.M. and Shock, E.L. (1997) Geochemical constraints on chemolithoautotrophic metabolism by microorganisms in seafloor hydrothermal systems. *Geochim Cosmochim Acta* **61**: 4375–91.

McDermott, J.M., Seewald, J.S., German, C.R., Sylva, S.P. (2015) Pathways for abiotic organic synthesis at submarine hydrothermal fields. *Proc. Natl. Acad. Sci. U. S. A.***112:** 7668-7672

Meyer, J.L., Akerman, N.H., Proskurowski, G., Huber, J.A. (2013) Microbiological characterization of post-eruption “snowblower” vents at Axial Seamount, Juan de Fuca Ridge. *Front Microbiol* **4**:153.

Osburn, M.R., Larowe, D.E., Momper, L.M., Amend, J.P. (2014) Chemolithotrophy in the continental deep subsurface : Sanford Underground Research Facility (SURF), USA. *Front Microbiol* **5**: 610.

Pruesse E, Quast C, Knittel K, Fuchs BM, Ludwig WG, Peplies J *et al* (2007). SILVA: a comprehensive online resource for quality checked and aligned ribosomal RNA sequence data compatible with ARB. *Nucleic Acids Res* **35:** 7188-7196.

Quast, C., Pruesse, E., Yilmaz, P., Gerken, J., Schweer, T., *et al.* (2013) The SILVA ribosomal RNA gene database project: improved data processing and web-based tools. *Nucleic Acids Res*. 41(Database issue): D590-D596.

Reeves, E.P., McDermott, J.M., and Seewald, J.S. (2014) The origin of methanethiol in midocean ridge hydrothermal fluids. *Proc. Natl. Acad. Sci. U. S. A.* **111**:5474-5479.

Schloss PD, Westcott SL, Ryabin T, Hall JR, Hartmann M, Hollister EB *et al* (2009). Introducing mothur: Open-Source, Platform-Independent, Community-Supported Software for Describing and Comparing Microbial Communities. *Appl Environ Microbiol* **75:** 7537-7541.

Shock, E.L., and Helgeson, C.H. (1988) Calculation of the thermodynamic and transport properties of aqueous species at high pressures and temperatures: Correlation algorithms for ionic species and equation of state predictions to 5 kb and 1000°C. *Geochim Cosmochim Acta* **52**: 2009–2036.

Shock, E.L., Helgeson, H.C., and Sverjensky, D.A. (1989) Calculation of the thermodynamic and transport properties of aqueous species at high pressures and temperatures : Standard partial molal properties of inorganic neutral species. *Geochim Cosmochim Acta* **53**: 2157–2183.

Shock, E.L., Sassani, D.C., Willis, M., and Sverjensky, D.A. (1997) Inorganic species in geologic fluids : Correlations among standard molal thermodynamic properties of aqueous ions and hydroxide complexes. *Geochim Cosmochim Acta* **61**: 907–950.

Shock, E.L. and Holland, M.E. (2004) Geochemical energy sources that support the subsurface biosphere. In The Subseafloor Biosphere at Mid-Ocean Ridges, Geophysical Monograph. Wilcock,W.S.D., DeLong,E.F., Kelley,D.S., Baross,J.., and Cary,S.C. (eds). American Geophysical Union, pp. 153–165.

Sverjensky, D.A., Shock, E. L., and Helgeson, H. C. (1997) Prediction of the thermodynamic properties of aqueous metal complexes to 1000°C and 5 kb. *Geochim Cosmochim Acta* **61**: 1359–1412.

Tamura K, Peterson D, Peterson N, Stecher G, Nei M, *et al.* (2011) MEGA5: molecular evolutionary genetics analysis using maximum likelihood, evolutionary distance, and maximum parsimony methods. *Mol Biol Evol* **28**: 2731–9.

Zinger, L., Amaral-Zettler, L. A., Fuhrman, J. A., Horner-Devine, M. C.,Huse, S. M.,Welch,D. B. M., et al. (2011) Global patterns of bacterial beta-diversity in seafloor and seawater ecosystems. PLoS ONE 6:e24570